Simultaneous nutrients (N,P) removal by using a hybrid inorganic sorbent impregnated with hydrated manganese oxide

Diana Guaya [a, b*], Cesar Valderrama [a], Adriana Farran [a], José Luis Cortina [a, c]

[a] Department of Chemical Engineering, Universitat Politècnica de Catalunya-Barcelona Tech (UPC), Barcelona, Spain

[b] Departament of Chemistry, Universidad Técnica Particular de Loja, Loja, Ecuador

[c] Water Technology Center CETaqua, Barcelona, Spain

*Correspondence should be addressed to: Diana Guaya

Department of Chemical Engineering, Universitat Politècnica de Catalunya, Av. Diagonal 647, 08028 Barcelona, Spain, Tel.: 93 4011818, Fax.: 93 401 58 14

Email: deguaya@utpl.edu.ec

Abstract

A natural clinoptilolite zeolite (Z-N) and its hybrid form (Z-Mn) prepared by impregnation with hydrated manganese oxide have been evaluated for the simultaneous removal of ammonium and phosphate. The ammonium sorption capacity reported by Z-Mn was 23±2 mg $N\text{-}NH_4^+$/g; while the phosphate uptake reached 5.6±0.2 mg $P\text{-}PO_4^{3-}$/g at pH 7.5. Both ammonium and phosphate uptake were slightly influenced coexisting ions commonly found in treated wastewater effluents. The Mn(II) activated zeolite (Z-Mn) improved the phosphate uptake capacity, in the pH range 7 to 9, by formation of surface complexes of P(V) anions with the precipitated Mn(II) hydrated oxide or by formation of mineral phases as Mn(II)--NH_4-PO_4 (e.g., $(NH_4MnPO_4 \cdot H_2O)$) which was detected by XRD analysis. The soil bio-availability test of loaded impregnated zeolites reported higher ammonium than phosphate bio-availability. The desorption of ammonium and phosphate from the loaded

manganese impregnated zeolites using 40 gL^{-1} NaOH solution in dynamic experiments reported higher recoveries and concentration factors of ammonium than phosphate.

Key words: clinoptilolite; sorption; hybrid sorbent; phosphate and ammonium recovery; hydrated manganese oxide

1. Introduction

Nitrogen (N) and phosphorus (P) based compounds are the major threats to natural water receiving bodies (e.g., rivers, lakes and oceans) as they provide suitable conditions for a fast and intensive growing of aquatic organisms and consequently their deterioration. N and P based compounds are found mainly in inorganic forms as ammonium and phosphate [1, 2], and in less extension organic species. New technologies are being studied for reduce their discharges to water bodies. Zeolitic materials have been used for ammonium removal from treated wastewater exhibiting sorption capacities from 0.3 to 2.1 mmol/g [3]. High efficiency has been demonstrated by zeolitic sorbents in the relative high presence of dissolved organic. Conversely, this condition limited the application of organic polymeric cation exchangers which conventionally developed capacities from 4 to 6 mmol/g for sulphonic resins [4, 5]. However, the main disadvantages of polymeric ion exchanger applied for tertiary urban or industrial effluents treatment are the low service volume and accordingly higher regeneration costs. Then, proposals have been addressed to: a) prepare low cost non-regenerable ammonium sorbents and then loaded ammonium sorbents could be used for agronomical application as could be improvement of soil quality in forest and degraded areas and b) improve properties to achieve the simultaneous ammonium and phosphate recovery to enhance their fertilizing properties. Taking zeolites as reference ammonium sorbent; a modification process of the zeolite to facilitate the sorption or the formation of P(V) mineral phases needs to be developed. In general oxyanions (e.g. As(V), P(V)) sorption could be achieved by using the complexing properties of the functional groups of hydrated metal oxides (HMOs). Metal oxides as Al(III), Fe(III), La (II) and Zr(IV) are known

sorbents for oxyanions through formation of inner-sphere complexes or Lewis acid-base (LAB) interactions [6, 7]. Anionic species, such as bicarbonate, chloride, sulfate or nitrate, exhibit poor sorption towards these hydrated metal oxides and can only form outer-sphere complexes with the metal oxides [8]. Application of granular Fe-HMO has been mainly restricted to remove low levels of As(V)/As(III) as single use sorbents to be disposed when exhausted due to the sorbates toxicity [9, 10]. However, when applied to non-toxic species as P(V), the loading capacities of granular Fe-HMO have tried to be implemented by increasing surface reactivity using HMO nanoparticles or by supporting them onto templates, such as clays [11], polymers [12] or zeolites [13].

Manganese oxides, widely applied to remove transition metals from water [14], have similar loading capacities for P(V) oxyanions but with weak complexation properties than Al and Fe oxides that could be suitable to develop a material providing neither efficient regeneration or high P(V) availability if applied as soil amendments.

The aim of this work was to evaluate the modification of a natural clinoptilolite zeolite by impregnation with hydrated manganese oxide to produce a hybrid sorbent and then assess its sorption performance for the simultaneous ammonium and phosphate removal. The specific objectives were:

(i) Characterize the natural and manganese modified hybrid sorbents prepared using a natural clinoptilolite.

(ii) Study the effect of both pH and competing ions (potassium, magnesium, calcium, sodium, bicarbonate, chloride, sulfate and nitrate) on the ammonium and phosphate sorption by natural clinoptilolite and manganese modified hybrid sorbent.

(iii) Study the effect of the initial concentration of ammonium and phosphate without and with the presence of competing ions (potassium, magnesium, calcium sodium, bicarbonate, chloride, sulphate, nitrate) on the sorption equilibrium of both the natural zeolite and manganese modified hybrid sorbent.

(iv) Evaluate the ammonium and phosphate kinetic by the manganese modified hybrid sorbent.

(v) Evaluate the release of the ammonium and phosphate from the manganese modified hybrid sorbent after the sorption process in a batch and dynamic systems

2. Materials and methods

2.1. Preparation of Na- and Mn- modified natural zeolites

A natural clinoptilolite zeolite (Z-N) from the Zeocem Company (Slovak Republic) was used in batch (particles < 200 μm) and fixed-bed (< 800 μm) experiments. Z-N was modified to the manganese form (Z-Mn) by using an adaptation of the method reported by Jiménez – Cedillo et al. [15]. Z-N samples (30 g) were first treated with 250 mL of 0.1 M NaCl and consecutively the formed sodium form (Z-Na) sample (30 g) was treated in 250 mL of $MnCl_2$ (0.1 M) by two consecutive times under reflux for 4 h obtaining Z-Mn. After treatment, samples were washed until no chloride was detected by the $AgNO_3$ test and dried at 80 °C for 24 hours.

2.2. Sorbents characterization before and after ammonium and phosphate sorption

The chemical composition and morphology of the samples were studied by a Field Emission Scanning Electron Microscope (JEOL JSM-7001F) coupled to an Energy Dispersive Spectroscopy system (Oxford Instruments X-Max). The test was replicated at least four times for each sample and the average values are reported. A powder X-ray Diffractometer (D8 Advance A25 Bruker) was used for X-ray diffraction (XRD) characterization of zeolitic samples. The infrared absorption spectra were recorded with a Fourier Transform FTIR 4100 (Jasco) spectrometer in the range of 4000 – 550 cm^{-1}. The nitrogen gas adsorption method was used to determine the sorbents specific surface area by an automatic sorption analyzer (Micrometrics). The tests were replicated at least four times for each sample and the average values are reported. Also, Z-N and Z-Mn samples (0.1 g) were equilibrated in 25 mL of solutions for different ionic strengths (deionized water; 0.01, 0.05 and 0.1 M NaCl) for 24 hours at 200 rpm and 21±1 °C. The point of zero charge (PZC) was determined by the pH drift

method in the range of pH 2 to 11 as described elsewhere [16]. Tests were performed in triplicate for each sample and the average values are reported.

2.3. Ammonium and phosphate sorption equilibrium studies

Batch equilibrium sorption experiments were carried out using standard methodology described elsewhere [17]. Weighted amounts of dry samples (particle size < 200 μm) were shaken overnight with 25 mL of aqueous solutions containing different phosphate and ammonium concentration. The solutions were prepared by dissolving $NaH_2PO_4.2H_2O$ and NH_4Cl in deionized water, respectively. The following types of experiments were performed.

2.3.1. Effect of pH on sorption

Z-Mn (0.1 g) samples were added to 25 mg P-PO_4^{3-}/L and 25 mg N-NH4+/L solutions at different pH values from 2 to 11.

2.3.2. Effect of competing ions

Z-Mn samples (0.1 g) were added to solutions (without pH adjustment) containing 25 mg P-PO_4^{3-}/L, 25 mg N- NH_4^+/L and 25 mg/L of the corresponding typical coexisting ions present in wastewater effluents.

2.3.3. Isotherms of ammonium and phosphate from a solutions without competing ions and with competing ions

The Z-N and Z-Mn samples (0.25 g) were equilibrated in solutions at pH 4.6±0.2 (without pH adjustment) and at pH 7.5±0.3 (with pH adjustment according to the expected treated wastewater conditions) using concentrations ranging 1 to 2000 mg P-PO_4^{3-}/L and 10 – 5000 mg N-NH_4^+/L.

The effect of the competing ions was evaluated through equilibration of Z-Mn sample (0.25 g) in solution containing concentrations ranging from 1 to 2000 mg P-PO_4^{3-}/L and 10 – 5000 mg N-NH_4^+/L. The composition of the solution was: sodium (260 mg/L), calcium (160 mg/L), magnesium (50 mg/L), potassium (40 mg/L), chloride (625 mg/L), bicarbonate (325 mg/L), sulfate (200 mg/L) and nitrate (30

mg/L). The ions concentrations were fixed taking as reference the average annual composition of the secondary effluent stream at the El Prat wastewater treatment plant (Barcelona – Spain).

2.3.4. Kinetic of the ammonium and phosphate sorption

Z-Mn (0.1 g) samples were equilibrated with 15 mg $N\text{-}NH_4^+$/L and 5 mg $P\text{-}PO_4^{3-}$/L (pH 6.4 and pH 7.5) solutions at room temperature (21±1 °C). Tubes were withdrawn sequentially at given times. Samples were centrifuged for 10 min and filtered (0.45 µm) before analysis and concentrations of ammonium and phosphate ions were determined. Also the loaded zeolites samples were examined by field scanning electron microscope and mineral phases were identified by X-Ray Diffractometry. All tests were performed by triplicate and the average values are reported.

2.4. Release of the ammonium and phosphate from manganese modified zeolite

2.4.1. Batch experiments

Z-Mn samples (0.5 g < 200 µm) were equilibrated in 25 mL of solution containing 25 mg $P\text{-}PO_4^{3-}$/L and 25 mg $N\text{-}NH_4^+$/L. The loaded sample was washed and dried; for being equilibrated into 25 mL of elution solutions: NaOH (1 M), $NaHCO_3$ (0.1 M), Na_2CO_3 (0.1 M), $NaHCO_3$/Na_2CO_3 (0.1 M). Tests were performed by triplicate (average values are reported) in two sorption – desorption cycles at 200 rpm and at 21±1 °C.

2.4.2. Column experiments

Z-Mn samples (<800 µm) were packed in a glass column (15mm x 100mm). The sorption was evaluated in presence and absence of competing ions through countercurrent flow rate of 2 mL/min. The expected values of the secondary effluent stream from the El Prat wastewater treatment plant (Barcelona – Spain) were considering for the feed composition: phosphate (13 mg/L), ammonium (25 mg/L), chloride (313 mg/L), bicarbonate (163 mg/L), sulfate (10 mg/L), nitrate (15 mg/L), sodium (130 mg/L), calcium (80 mg/L), magnesium (25 mg/L) and potassium (20 mg/L). After, Z-Mn was saturated it was regenerated using 1 M NaOH solution at flow rate of 0.5 mL/min.

2.5. Sequential chemical fractionation of phosphorus

An adapted sequential extraction method from Hieltjes and Lijklema [18] was used for the fractionation of immobilized phosphorus in loaded zeolite. Z-Mn sample (0.25 g) was equilibrated in 25 mL of 25 mg P-PO_4^{3-}/L solution. The first stage involves two consecutive extractions in 20 mL of 1 M NH_4Cl (pH 7) for the loosely bound phosphorus fraction (LB-P) determination. The iron, aluminum and manganese fraction (Fe+Al+Mn)-P was extracted two consecutive times in 20 mL of 0.1 M NaOH followed by extraction in 1 M NaCl. Finally, two consecutive extractions in 20 mL of 0.5 M HCl determined the phosphorus bound to calcium, magnesium and manganese compounds (Ca+Mg+Mn)-P. The residual phosphorus (R-P) was calculated by the mass balance between the phosphorus adsorbed and the extracted fractions. Tests were performed by triplicate at 21±1 °C and average data are reported.

2.6. Ammonium and phosphate analysis

Standard Methods were used for ammonium (N) and phosphate (P) quantification [19]. The P concentration was analyzed by the vanadomolybdophosphoric acid colorimetric method (4500-P C) and N concentration was determined by ammonia-selective electrode method (4500-NH3 D). Also, it was used a Thermo Scientific Ionic Chromatograph (Dionex ICS-1100 and ICS-1000) for ions determination.

3. Results and discussions

3.1. Characterization of modified zeolite before and after ammonium and phosphate sorption

The chemical composition for clinoptilolite included O, Na, Mg, Al, Si, K, Ca and Fe (Table 1). The FSEM – EDX data and the analysis of aqueous phase (data not reported) suggested the occurrence of ion exchange reactions when manganese form of zeolite were obtained by the releasing of Na^+,

K^+, Mg^{2+} and Ca^{2+} ions. Then, the modification of the Z-Na to Z-Mn could be described as a partial cation exchange reaction described by Eq. 1-2:

$$2\ (\cong ZO^-Na^+/K^+) + Mn^{2+} \rightleftarrows (\cong ZO^-)_2Mn^{2+} + 2Na^+/K^+ \quad (1)$$

$$2\ (\cong ZO^-)Ca^{2+}/Mg^{2+} + Mn^{2+} \rightleftarrows (\cong ZO^-)_2Mn^{2+} + Ca^{2+}/Mg^{2+} \quad (2)$$

Element	Z-N	Z-Na	Z-Mn	Loaded Z-Mn
O	57.8±2.6	60.3±1.4	59.8±2.6	58.9±3.2
Na	0.3±0.0	1.5±0.1	1.2±1.5	0.4±0.1
Mg	0.4±0.1	0.4±0.0	0.1±0.1	0.1±0.1
Al	5.3±0.2	5.3±0.0	6.3±1.9	5.3±0.3
Si	29.7±1.7	29.1±1.5	27.4±1.7	32.7±2
P	<lq*	<lq*	<lq*	0.3±0.1
Cl	<lq*	<lq*	<lq*	<lq*
K	2.9±0.5	1.8±0.2	1.4±0.5	0.9±0.5
Ca	1.9±0.3	1.1±0.1	1.3±0.9	0.3±0.1
Ti	0.2±0.2	<lq*	<lq*	<lq*
Mn	<lq*	<lq*	1.6±1.1	0.3±0.14
Fe	1.60±0.4	0.5±0.0	0.9±0.5	0.9±0.5

lq*: limit of quantification

Table 1. Chemical composition (FSEM – EDX, wt. %) of Natural zeolite (Z-N), zeolite in sodium form (Z-Na), zeolite in manganese form (Z-Mn) and loaded zeolite in manganese form (Loaded Z-Mn).

Clinoptilolite showed the typically networks of crystal clusters plate-like morphology, as can be seen in FSEM-EDAX analysis (Supplementary material Figure S1a). The Z-Na and Z-Mn particles surfaces were covered with small crystals (Supplementary material Figure S1 b, c) and a reduction of the specific surface area from 19.8±0.8 m^2/g for Z-N to 17.6±0.9 m^2/g in Z-Mn was measured, as has been described elsewhere [20].

The Z-N, Z-Na and Z-Mn were mainly composed by clinoptilolite and traces of albite and quartz (Supplementary material Figure S2) and no important changes were identified by the exchange of Mn^{2+} by Na+ ions and/or the subsequent precipitation of manganese oxide on the exchange sites of the zeolitic structure. The absence of crystalline phases was confirmed in Z-Mn as it was reported for a natural zeolite in the iron and manganese form [21, 22]. Moreover, the pH_{pzc} of Z-Mn sample was 6.1±0.6, which is in agreement with those values reported for a natural MnO_2 (pH_{pzc} 5.5) and for Mn(II) and Mn(IV) hydroxy/oxides and some natural MnO_2(s) (pH_{pzc} 4.0±0.8) [23, 24]. However it was slightly far from 7.0 and 8.7 described for β-MnO_2(s) and crystalline MnO_2, respectively [25, 26].

Bands between 798 cm^{-1} and 547 cm^{-1}, at ~1100 cm^{-1} and at ~1630 cm^{-1} corresponding to the deformation vibration of OH, Al-O-Si and Si-O-Si groups, stretching vibration of Si–O groups and the deformation vibration of water, respectively were observed on the FTIR spectra of Z-N, Z-Na and Z-Mn (Supplementary material Figure S3). Some differences between Z-N and Z-Mn spectra were found in the bands from 3700 cm^{-1} to 3100 cm^{-1} which correspond to the zeolite hydroxyl groups [27, 28], and the sorbed water molecules responsible for metal ions sorption [29]. New bands were found in Z-Mn at 1396 cm^{-1}, 1455 cm^{-1} and 1541 cm^{-1} and at 3747 cm^{-1} which correspond to the bridging hydroxyl groups (Si-OH-Mn) [30, 31]; then this fact suggested the existence of hydrated oxide manganese covering the clinoptilolite surface Z-Mn as it was determined by the SEM images.

3.2. Ammonium and phosphate sorption

3.2.1. Effect of pH on ammonium and phosphate sorption

The ammonium and phosphate sorption on the manganese HMO impregnated zeolites occurs through chemical and physical interactions [32].

The ammonium sorption by Z-Mn increases from pH 2 until 4 and then is maintained constant until pH 10 (Figure 1). The existence of positive charges on Z-Mn below pH_{Ppzc} promotes competition for the ammonium removal while above the pH_{pzc} the ammonium sorption is governed by the

electrostatic interaction with the HMO deprotonated surface groups (≅MnO^-). Thus, the decrease of ammonium sorption at pH 11 is associated with the decrease of the NH_4^+ concentration as it is converted to the NH_3. The analysis of aqueous phase (data not reported) and the SEM analysis confirmed the release of Na^+ and in less degree of K^+, Mg^{2+} and Ca^{2+} in the loaded Z-Mn. Moreover, EDAX revealed an important reduction of manganese content in the loaded ammonium and phosphate Z-Mn zeolite after the ammonium sorption (Table 1). So ammonium also could be exchanged by Mn2+ cations from the zeolite network. Then, the ion exchange reaction on a manganese oxide impregnated zeolite is a chemical process involving valence forces through electrons between zeolite sites with negative charge and ammonium cations as described by Eq. 3 [33]:

$$(\cong ZO^-)_2Mn^{2+} + 2NH_4^+ \rightleftarrows 2(\cong ZO^-NH_4^+) + Mn^{2+} \quad (3)$$

A low phosphate sorption capacity was reported between pH 2 and pH 6 (Figure 1), which is mainly governed by electric interaction where the surface of hydrated manganese oxide groups of Z-Mn were possitively-charged below pH_{pzc}= 5.4 as described by Eq. 4.

$$\cong MnOH^+ + H_2PO_4^- \rightleftarrows (\cong MnOH^+H_2PO_4^-) \quad (4)$$

where ≅MnOH represents the surface groups of the hydrated manganese oxide precipitated on the zeolite structure.

Contrary, the phosphate sorption capacity increased from pH 7 to pH 9 in Z-Mn charged negatively; then the sorption of the expected phosphate oxyanion forms, $H_2PO_4^-$ and HPO_4^{2-} were mainly achieved by ligand exchange complexation with the hydroxyl surface groups [34] through inner sphere complexation [35] as described by Eq. 5.

$$\cong MnOH + H_2PO_4^-/HPO_4^{2-} \rightleftarrows \cong MnH_2PO_4^-/HPO_4^2 + OH^- \quad (5)$$

Sorption experiments were also characterized for the formation of precipitates on the surface of the Z-Mn between pH 7 to 9, and it was detected visually with a change of zeolite from pale grey to browner color. The XRD patterns of the loaded Z-Mn samples revealed the existence of new crystalline phase ammonium manganese phosphate hydrate oxide ($NH_4MnPO_4 \cdot H_2O$) (Supplementary material Figure S2). Then, precipitation is an additional mechanism proposed for phosphate sorption on Z-Mn due to the formation of some (P(V) – Mn^{2+} – NH_4^+ - Ca^+/ Mg^{2+}/ Na^+/ K^+ complexes [36] as described by Eq. 6 -7:

$$(\cong ZO^-)_2Mn^{2+} + HPO_4^{2-} + 2Na^+ \rightleftarrows 2\,(\cong ZO^-Na^+) + MnHPO_4(s) + H^+ \quad (6)$$

$$(\cong ZO^-)_2Mn^{2+} + HPO_4^{2-} + 2Na^+ + NH_4^+ \rightleftarrows 2\,(\cong ZO^-Na^+) + NH_4MnPO_4(s) + H^+ \quad (7)$$

It should be mention that the Na and Mn contents on Z-Mn are in the same order of magnitude (Table 1).

Above pH 10 the conversion of HPO_4^{2-} into PO_4^{3-} form promotes the reduction of phosphate sorption capacity by effect of repulsion with the negative charges of the impregnated zeolite surface. Furthermore, in these pH conditions the formation of the mixed metal ($Mn/NH_4/PO_4$) mineral is not favoured as it was described for the $MnHPO_4(s)$ and $Mn_3(PO_4)_2(s)$.

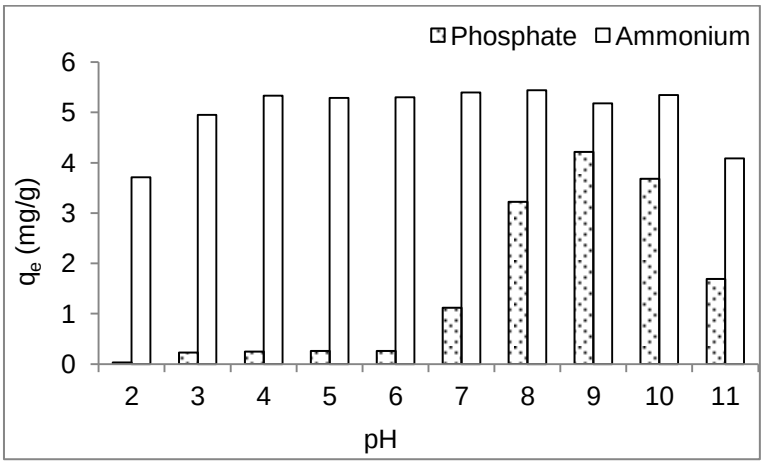

Figure 1. Effect of pH on the ammonium and phosphate sorption capacity by Z-Mn.

3.2.2. Effect of the competing ions

The ammonium and phosphate removal was evaluated in the presence of common cationic species in wastewater effluents (Figure 2). The ammonium uptake by Z-Mn was affected by the presence of Ca^{2+} (20 %) > K^{+} (14 %) > Na^{+} (10 %) > Mg^{2+} (7 %); as was reported for other natural zeolites [33]. The phosphate sorption was slightly improved as it was reported for MnO_2 surfaces in combination of alkaline earth cations [36]; however, although detected by FSEM-EDAX, the XRD analysis did not reveal the precipitation of Ca^{2+}/ Mg^{2+}-phosphate species [37].

The ammonium and phosphate sorption was not affected by the presence of anions. It is in accordance with the effects reported for ammonium and phosphate removal in the presence of chloride and sulfate rich solutions [5, 33]; while the outer-sphere complexation of these species result in the permanent availability of phosphate bonding sites [8]. It should be pointing out that the significant increase of phosphate sorption in the presence of high concentrations of HCO_3^- (characterized by pH values ~7), which enhances the phosphate sorption on manganese modified hybrid sorbent [36]. Otherwise, a reduction of 14 % of ammonium sorption capacity was found in the multi anions solution.

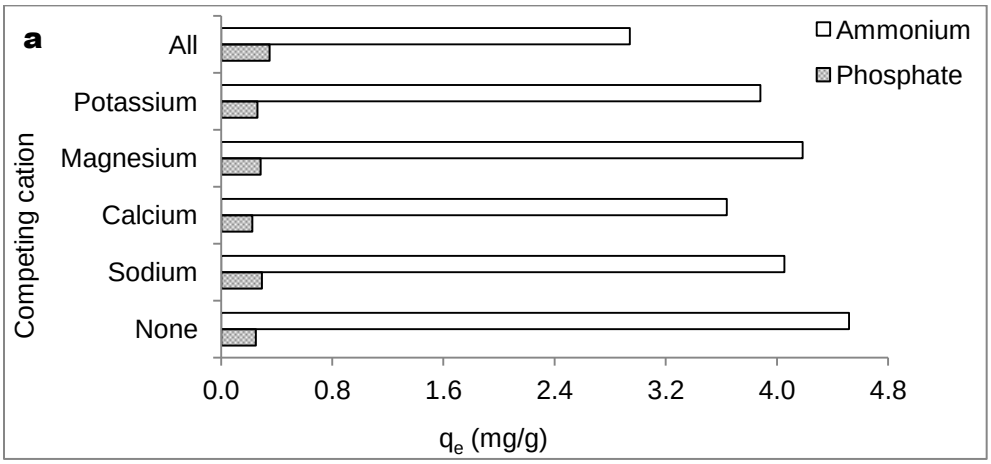

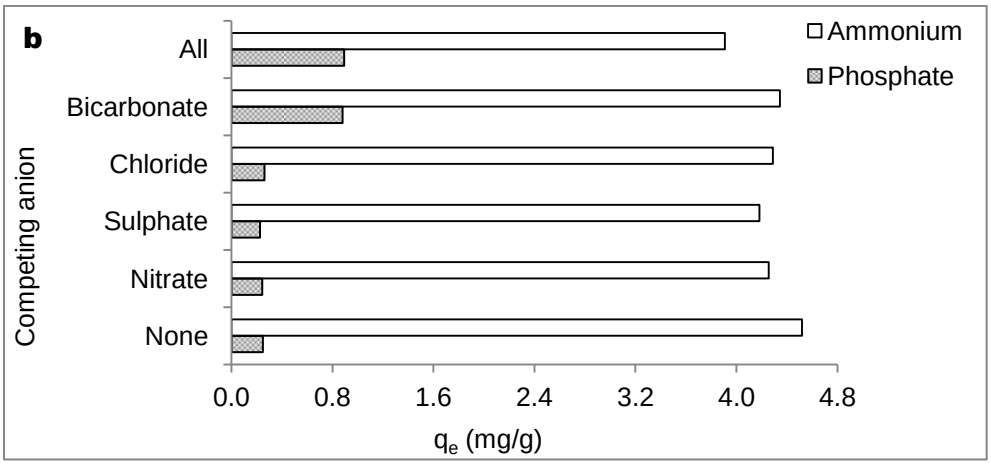

Figure 2. Individually effect of a) cations and b) anions on ammonium (N) and phosphate (P) uptake by manganese zeolite (Z-Mn).

3.2.3. Isotherms of ammonium and phosphate from solutions without competing ions and with competing ions

The equilibrium uptake for ammonium and phosphate (q_e) was calculated by Eq. 8.

$$\boldsymbol{q_e = (C_o - C_e) \times \frac{v}{w}} \quad (8)$$

where C_o (mg/L) and C_e (mg/L) represent the initial and equilibrium concentrations, respectively; v (L) is the aqueous solution volume and w (g) is the mass of impregnated zeolite. The ammonium and phosphate equilibrium sorption was evaluated according to Langmuir (Eq. 9) and Freundlich (Eq. 10) isotherms.

$$\boldsymbol{\frac{C_e}{q_e} = \frac{1}{K_L . q_m} + \frac{C_e}{q_m}} \quad (9)$$

$$\boldsymbol{\log q_e = \log K_F + \frac{1}{n} log\ C_e} \quad (10)$$

where q_m (mg/g) is the maximum sorption capacity and K_L (L/mg) is the Langmuir sorption equilibrium constant. K_F ((mg/g)/(mg/L)$^{1/n}$) is the Freundlich equilibrium sorption constant.

The equilibrium data of ammonium and phosphate sorption by manganese modified hybrid sorbent was better described by the Langmuir isotherm. The R^2 values are 0.99 (Table 2), proving that the experimental sorption data was appropriated described by this model. Thus, monolayer and homogenous ion exchange and/or sorption at specific and equal affinity sites available on the impregnated zeolites surface is supposed to occur. Moreover, the separation factor R_L or equilibrium parameter was calculated by Eq. 11, which provides an insight of the nature of adsorption. Lower R_L values were determined, 0.05 and 0.02 for phosphate and ammonium, respectively, indicating that adsorption is favorable ($0 < R_L < 1$) [38].

$$\mathbf{R_L} = \frac{\mathbf{1}}{(\mathbf{1}+K_L C_o)} \qquad (11)$$

pH_{eq}	Zeolite	Ion specie	Langmuir			Freundlich		
			q_m (mg/g)	K_L (L/mg)	R^2	K_F ((mg/g)/(mg/L)$^{1/n}$)	1/n	R^2
	Z-N	Phosphate	0.6±0.1	0.01	0.99	0.02	0.47	0.97
		Ammonium	33±2	0.006	0.99	1.84	0.36	0.94
4.6±0.2	Z-Mn	Phosphate	2.8±0.4	0.01	0.99	0.30	0.32	0.96
		Ammonium	31±3	0.009	0.99	2.63	0.34	0.85
7.5±0.3	Z-Mn	Phosphate	5.6±0.3	0.01	0.99	0.95	0.34	0.65
		Ammonium	23±2	0.01	0.99	2.50	0.29	0.93

Table 2. Isotherm parameters for ammonium and phosphate sorption on Z-N and Z-Mn.

The Z-N reported maximum sorption capacities (q_m) of 33±2 mg $N\text{-}NH_4^+$/g and 0.6±0.1 mg $P\text{-}PO_4^{3-}$/g for ammonium and phosphate, respectively; as it was described in a previous study [39]. For the manganese modified hybrid sorbent ammonium sorption capacity decreased from 31±3 mg $N\text{-}NH_4^+$/g

(at pH 4.6) to 23±2 mg N-NH_4^+/g (pH 7.5) (Table 2); while the phosphate removal capacity increased from 2.8±0.4 mg P-PO_4^{3-}/g (at pH 4.6) up to 5.6±0.3 mg P-PO_4^{3-}/g (pH 7.5). The experimental equilibrium isotherms for ammonium and phosphate removal by manganese zeolite are shown in Figure 3. The increase of phosphate removal between pH 6 and 9 is due to the interaction of the hydrous manganese (IV) oxide (HMO) and alkaline earth cations [36]; as it was confirmed by the XRD patterns of the loaded Z-Mn samples (Ammonium Manganese Phosphate Hydrate Oxide, $NH_4MnPO_4 \cdot H_2O$). The existence of phosphorous and nitrogen was confirmed in loaded zeolite Z-Mn, and the surface was covered by a solid crystalline framework (Supplementary material Figure S1d). However, it could not be discarded the presence of Mn-PO_4 minerals (e.g., $MnHPO_4$(s), $Mn_3(PO_4)_2$(s)). The FTIR spectra revealed important changes in bands at 3747 cm^{-1}, 1016 cm^{-1} and 1435 cm^{-1}; which correspond to the hydroxyl groups complexed with ammonium and phosphate [40, 41]. This fact could explain that the increase of the phosphate removal leads to the slight reduction of the ammonium sorption capacity as it occurred in both the natural and in the manganese modified hybrid sorbent zeolite forms.

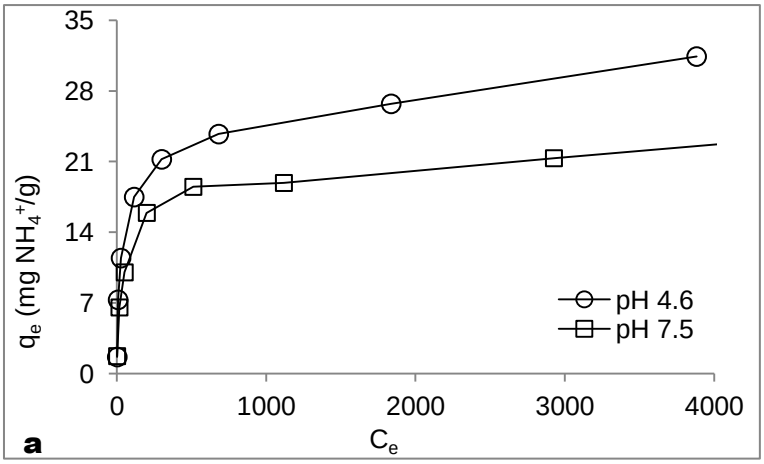

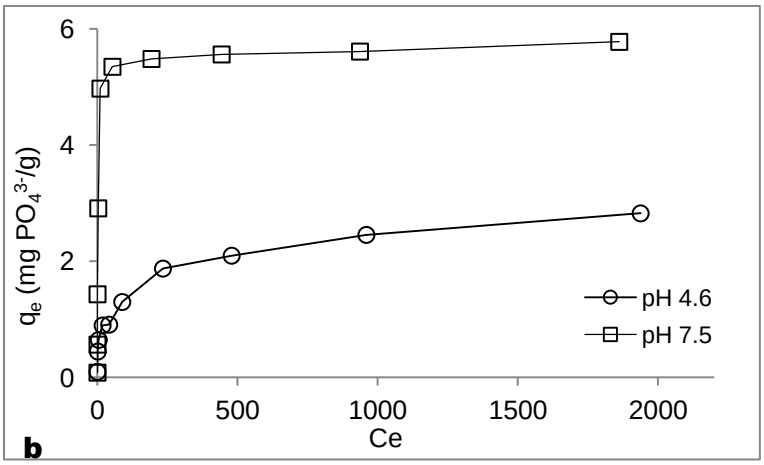

Figure 3. Experimental equilibrium isotherms for a) ammonium and b) phosphate removal by manganese zeolite (Z-Mn) at 21±1°C. Sorption experiments were carried at constant equilibrium pH 4.6±0.2 and 7.5±0.3.

Ammonium and phosphate equilibrium sorption data on Z-Mn in the presence of mixtures of anions and cations were also better described by the Langmuir isotherm. The R^2 values equal to 0.99 (Table 3) demonstrated that experimental sorption data was well described by this model. Also, R_L values between 0 and 1 for phosphate and ammonium indicates that adsorption is highly favoured.

The phosphate uptake capacity was slightly reduced in the presence of all ions (3.3±0.3 mg P-PO_4^{3-}/g at pH 5.1 ±0.2) and cations (2.7±0.2 mg P-PO_4^{3-}/g at pH 5.1 ±0.2) while in the presence of anions it was increased to 3.6±0.3 mg P-PO_4^{3-}/g (pH 6.5±0.2) as the pH increases (Table 3). Similar effect was reported for ammonium uptake in the presence of cations mixture (26±2 mg N-NH_4^+/g) > cations and anions mixture (27±2 mg N-NH_4^+/g) > anions mixture (27±3 mg N-NH_4^+/g).

pH_{eq}	Ion specie	Langmuir			Freundlich		
		q_m (mg/g)	K_L (L/mg)	R^2	K_F ((mg/g)/(mg/L)$^{1/n}$)	1/n	R^2

4.6±0.2	Phosphate	2.8±0.4	0.01	0.99	0.30	0.32	0.96
6.5 ±0.2	P-Anions	3.6±0.3	0.01	0.99	0.82	0.31	0.48
5.1 ±0.2	P-Cations	2.7±0.2	0.01	0.99	0.44	0.24	0.99
5.1 ±0.2	P-Ions	3.3±0.3	0.01	0.99	0.49	0.38	0.82
4.6 ±0.2	Ammonium	31±3	0.009	0.99	2.63	0.34	0.85
6.5 ±0.2	N-Anions	27±3	0.013	0.99	2.03	0.36	0.86
5.1 ±0.2	N-Cations	26±2	0.008	0.99	1.20	0.42	0.79
5.1 ±0.2	N-Ions	27±2	0.005	0.99	0.82	0.47	0.89

Table 3. Isotherm parameters for ammonium and phosphate sorption on manganese impregnated zeolite Z-Mn in the presence of competing ions.

The ammonium and phosphate removal from aqueous solutions have been widely studied, a comparison of the loading capacity of various materials with those obtained in the present study is summarized in Table 4.

Sorbent	Description	System		NH_4^+ q_e (mg/g)	PO_4^{3-} q_e (mg/g)	Langmuir isotherm parameters NH_4^+ q_m (mg/g)	NH_4^+ K_L (L/mg)	PO_4^{3-} q_m (mg/g)	PO_4^{3-} K_L (L/mg)	Ref.
Natural zeolite	Hydrated manganese oxide impregnated clinoptilolite pH 7-8	Static	Single Multi-component	20 24	5 3	23 27	0.01 0.005	5.6 3.3	0.01 0.01	This study
		Dynamic	Single Multi-component	21 17	7.4 5.2	-	-	-	-	
Natural zeolite	Hydrated aluminium oxide impregnated clinoptilolite	Static	Single Multi-component	28 21	6.7 5.8	30 26	0.01 0.007	7.0 6.3	0.02 0.02	[39]
		Dynamic	Single Multi-component	28 16	5 3	-	-	-	-	
Natural zeolite	Hydrated iron oxide impregnated clinoptilolite	Static	Single Multi-component	24 20	3.0 2.8	27 23	0.004 0.002	3.4 3.1	0.02 0.02	[42]
		Dynamic	Single Multi-component	26 15	2.7 1.1	-	-	-	-	
Coal fly ash	Coal fly ash from thermoelectric power plants, composed by mullite and quartz	Static	Single	-	-	2.2	0.06	4.1	0.001	[43]
Synthetic zeolite	Zeolite synthesized from fly ash via alkaline hydrothermal treatment, composed by mullite	Static	Single	-	-	34.5	0.001	26.8	0.004	
Natural zeolite	Turkish zeolite composed by clinoptilolite/heulandite, mordenite and quartz	Static	Single	-	-	9.64	0.05	-	-	[44]

Natural zeolite	Clinoptilolite treated with different sodium concentrations in millimeter and nanometer particle sizes	Static	Single	-	-	10.3 to 11.5	0.0003 to 0.02	-	-	[45]
Natural zeolite	Clinoptilolite	Static	Single	-	-	3.45	0.2	-	-	[46]
Natural zeolite	Activated in aqueous solution of sodium chloride	Static	Single	-	-	9.5 to 9.7	0.1 to 0.4	-	-	
Synthetic zeolite	Zeolite was synthetized from fly ash and it was composed by zeolite X (faujasite), zeolite A, zeolite P	Static	Single	-	-	30 to 37	0.006 to 0.01	-	-	[5]
Natural zeolite	Australian natural zeolite composed by quartz, clinoptilolite sodium and calcium and modernite	Static	Single	-	-	6.30	0.05	-	-	[47]
Natural zeolite	Ukraine zeolite composed mainly by clinoptilolite. The zeolite was treated with 2 M solutions of HCl and NaCl	Static	Single	6.8	-	-	-	-	-	[48]
		Dynamic	Single Multi-component	13.6 to 21.5	-	-	-	-	-	
Clay material	Mesolite as ion exchange medium for ammonium removal	Dynamic	Single	47 to 51	-	-	-	-	-	[49]
Titanium mesostructure	Mesostructure based on an inorganic material (titanium)	Static	Single	-	49.3	-	-	51.2	0.013	[50]

Polymeric ion exchanger	FIBAN-As, Fibrous ion exchanger impregnated with nanoparticles of hydrated ferric oxide (HFO)	Static	Single Multi-component	-	-	-	-	162 156	0.009 0.003	[51]
		Dynamic	Single Multi-component	-	48.1 9.8	-	-	-	-	
Polymeric ion exchanger	FO36, weak base anion exchanger resin impregnated with hydrated ferric oxide (HFO)	Static	Single Multi-component	-	-	-	-	91.3 89	0.007 0.008	[52]
Natural sepiolite	Chinese calcium rich sepiolite	Static	Single	-	32	-	-	-	-	[53]
Synthetic zeolite	Zeolite in the sodium form synthetized from coal fly ash composed by mullite and quartz	Static	Single	-	-	-	-	153 to 204	0.004	[54]
	Zeolite in the calcium form synthetized from coal fly ash composed by mullite, quartz, calcite, garronite	Static	Single	-	-	-	-	43 to 57	0.0004 to 0.0006	
Natural clays	Clay samples from Tunisia composed by illite, kaolinite, smectite, quartz and calcite.	Static	Single	-	-	-	-	38 to 42	0.02	[55]
Synthetic zeolite	Synthetized zeolite A from natural clay by conventionally fusion method	Static	Single	-	-	-	-	53	0.03	
Natural bentonite	Iranian bentonite sample composed by montmorillonite and quartz	Static	Single	-	-	-	-	0.4	0.01	[56]

Natural kaolinite	Iranian kaolinite sample composed by chlorite, illite, kaolinite feldspar, quartz	Static	Single	-	-	-	-	0.6	0.005	
Natural zeolite	Iranian zeolite sample composed by clinoptilolite, chlorite, kaolinite, feldspar, quartz	Static	Single	-	-	-	-	0.6	0.007	

Table 4. Comparison of ammonium and phosphate sorption capacity data by various sorbents materials and values obtained in this study.

3.2.4. Kinetic of the ammonium and phosphate sorption

The sorption kinetics of both the ammonium and phosphate ions on Z-Mn, revealed that equilibrium was reached within 100 to 200 minutes (Figure 4). The phosphate sorption capacities were lower at pH 6.2 compared with that obtained at pH 8.0; while the opposite effect was revealed in ammonium ions.

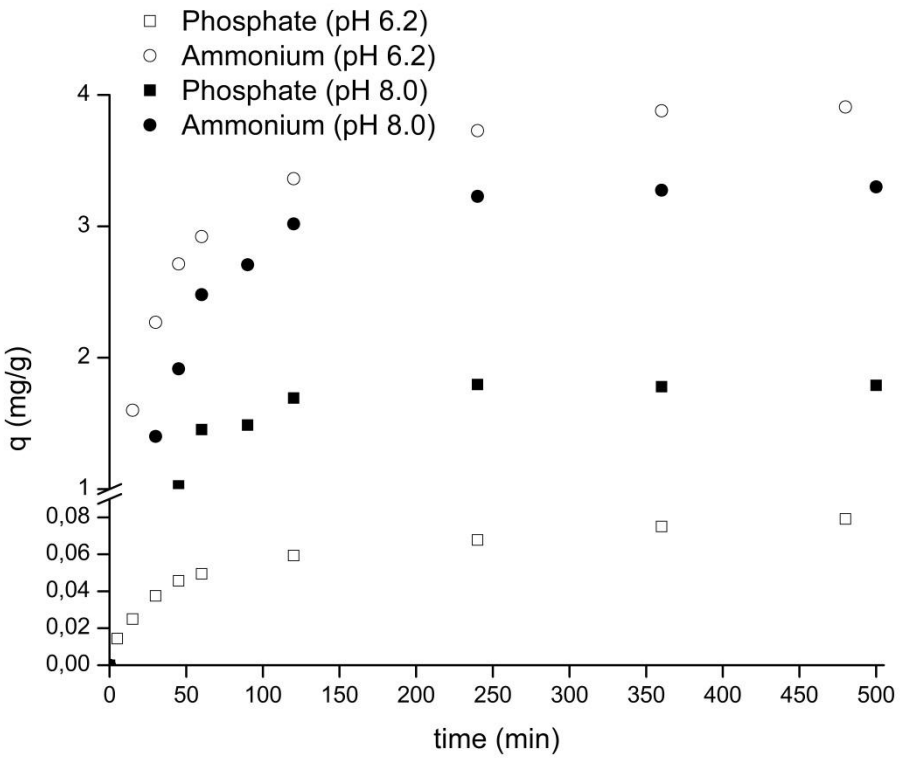

Figure 4. Evolution of ammonium and phosphate sorption uptake versus time for Z-Mn at 21 ±1 ºC.

The ammonium and phosphate equilibrium sorption kinetics were well described by the intraparticle diffusion model (Eq. 12) [57]; which considers the sorbate is transported from the bulk solution to the external surface of impregnated zeolite and posterior diffusion in the interior particles governed the sorption mechanisms.

$$q_t = k_t\, t^{1/2} + A \qquad (12)$$

where A (mg/g) is a constant providing information about the thickness of the boundary layer and k_t (mg.g^{-1}.h$^{-1/2}$) is the intraparticle diffusion rate constant. Two linear regions were identified when experimental data was fitted to this kinetic model, suggesting that the ammonium and phosphate sorption process could be described by film diffusion followed by particle diffusion process [58].

The homogenous particle diffusion model (HPDM) was used to describe the kinetic sorption data [59, 60]. If particle diffusion controls (Dp) the sorption rate is described using Eq. 13:

$$-\ln\left(1-\left(\frac{q_t}{q_e}\right)^2\right)=\frac{2\,\pi^2 D_p}{r^2}t \qquad (13)$$

When the rate of sorption is controlled by liquid film diffusion, it is expressed by Eq. 14:

$$-\ln\left(1-\left(\frac{q_t}{q_e}\right)\right)=\frac{D_f C_s}{h\,r\,C_z}t \qquad (14)$$

where q_t and q_e are the solute loadings on the adsorbent phase at time t and equilibrium (mg/g), respectively, t is the contact time (min), C_s (mg/L) and C_z (mg/kg) are the ion concentrations in solution and in the zeolite, respectively, r is the average radius of the zeolite particles (1x10^{-4} m), and h is the thickness of film around the zeolite particle [61]. D_p is the diffusion coefficient in the zeolite phase (m^2.s^{-1}) and D_f (m^2.s^{-1}) is the diffusion in the film phase surrounding the zeolite particles.

Ammonium and phosphate sorption kinetic data on Z-Mn were fitted to the equations 12, 13 and 14 and the best-fit of D_p and D_f values as well as the linear regression analysis are summarized in Table 5. Higher regression coefficient (R^2) values were found for particle diffusion; therefore this is the rate limiting step for ammonium and phosphate sorption. The good correlation with the particle diffusion model could be explain in terms of the ammonium exchange with the sodium ion of impregnated zeolite, as it was reported by Sprynskyy (2005) [62]; and the relation of ligand exchange complexation of phosphate with the hydroxyl surface groups of the impregnated zeolite.

Model	Kinetic parameters	Ammonium		Phosphate	
		pH 6.4±0.2	pH 8.0±0.2	pH 6.2±0.2	pH 8.0±0.2
Intraparticle diffusion	k_t ($mg \cdot g^{-1} \cdot h^{-1/2}$)	1.28	1.31	0.03	0.71
	R^2	0.90	0.80	0.90	0.77
HPDF Film diffusion	D_f ($m^2 \cdot s^{-1}$)	$1.9x10^{-9}$	$1.8x10^{-9}$	$7.8x10^{-11}$	$4.5x10^{-9}$
	R^2	0.91	0.84	0.94	0.78
HPDM Particle diffusion	D_p ($m^2 \cdot s^{-1}$)	$3.0x10^{-12}$	$8.8x10^{-12}$	$1.7x10^{-12}$	$9.5x10^{-12}$
	R^2	0.96	0.98	0.99	0.98

Table 5. Kinetic parameters for ammonium and phosphate removal on Z-Mn at 21 ±1 ºC.

3.3. Release of the ammonium and phosphate from manganese modified zeolite

3.3.1. In a batch system

Availability of ammonium and phosphate was studied in both strong moderate alkaline solutions bicarbonate and free bicarbonate solutions. Ammonium was efficiently desorbed in strong basic solutions (pH> 12 as 1M NaOH 0.1 M and 0.1 M Na_2CO_3) and partially removed by slightly basic solutions (e.g. pH> 8 as 0.1 M $NaHCO_3$, 0.1 M $NaHCO_3$/0.1 M Na_2CO_3 (pH= 10.3)) (Table 6).

Elution solution	Desorption (%)	
	Ammonium	Phosphate
1 M NaOH (pH>13)	89±4	90±3
0.1 M $NaHCO_3$ (pH=8.3)	41±4	34±3
0.1 M Na_2CO_3 (pH=11.8)	83±4	33±3
0.1 M $NaHCO_3$/0.1 M Na_2CO_3 (pH=10.3)	64±4	72±3

Table 6. Simultaneous ammonium and phosphate desorption efficiency from loaded Z-Mn at 21±ºC.

In concentrated Na^+ and OH^- containing solutions Eq 3 is reversed as NH_4^+ ions are additionally converted to NH_3 as described by Eq. 15.

$$ZO^-NH_4^+ + Na^+ + OH^- \cong \rightleftarrows \cong ZO^-Na^+ + NH_3 + H_2O \quad (15)$$

However only partial recoveries are measured in more diluted solutions or at pH values where the formation of NH_3 is not favoured.

Phosphate is only efficiently desorbed in 1M NaOH solutions and partially desorbed in the $NaHCO_3/Na_2CO_3$ mixtures. Partial desorption of phosphate could be explained when using $NaHCO_3$, Na_2CO_3 and $NaHCO_3$/ Na_2CO_3 solutions by Eqs. 16 and 17:

$$\cong MnOH^+H_2PO_4^- + 2OH^- \rightleftarrows \cong MnO^- + PO_4^{3-} + 2H_2O \quad (16)$$

$$\cong MnH_2PO_4^-/HPO_4^{2-} + OH^- \rightleftarrows \cong MnO^- + PO_4^{3-} \quad (17)$$

The desorption of more stable phosphate species (e.g., mineral phases found on the zeolite structure) and only favoured in strongly basic solutions are described by Eqs. 18 and 19.

$$MnHPO_4(s) + OH^- \rightleftarrows \cong MnO^- + PO_4^{3-} + H_2O \quad (18)$$

$$NH_4MnPO_4(s) + OH^- \rightleftarrows + PO_4^{3-} + Mn^{2+} + NH_3 + H_2O \quad (19)$$

In the subsequent sorption cycles the regenerated Z-Mn samples ($NaHCO_3$, Na_2CO_3 and $NaHCO_3$/ Na_2CO_3) shown a strong decrease in phosphate uptake in comparison with the ammonium removal capacity. No previous studies have been reported about a modified zeolite Z-Mn for ammonium and phosphate removal considering the regeneration step. However, the results obtained suggest that zeolite should be impregnated after each regeneration cycle or could be used for the improvement of soil quality.

3.3.2. Sorption column experiments

The ammonium maximum sorption capacity at column saturation (C/C_0=0.95) was 28 mg N-NH_4^+/g at 416 BV (pH 6.0) and 21 mg N-NH_4^+/g at 424 BV (pH 8.0), while in the presence of competing ions, the ammonium maximum sorption capacity decreased to 17 mg N-NH_4^+/g at 400

BV (pH 7.0) (Figure 5). In addition, the phosphate maximum sorption capacity increased from 0.4 mg P-PO_4^{3-}/g at 167 BV (pH 6.0) to 7.4 mg P- PO_4^{3-}/g at 167 BV (pH 8.0), while in the presence of coexisting ions it was 5.2 mg P-PO_4^{3-}/g at 400 BV (pH 7.0).

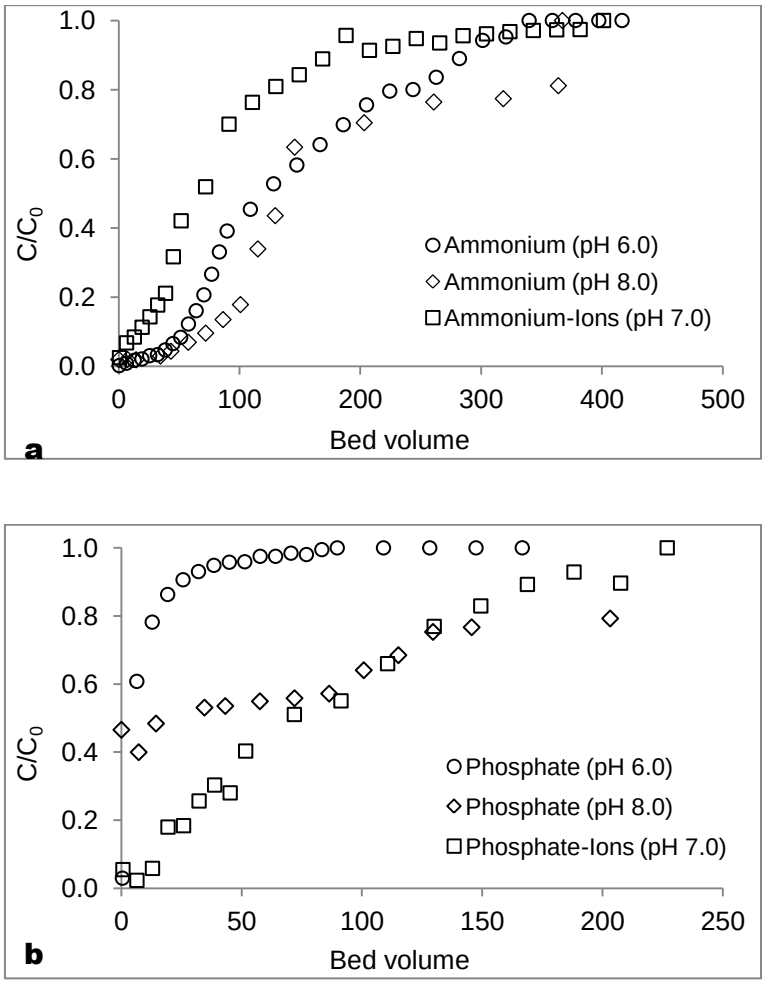

Figure 5. Breakthrough curves of a) ammonium and b) phosphate uptake by manganese zeolite (Z-Mn) at flow rate of 1.8 mL/min.

After desorption experiments it was recovered 90 % of ammonium and 60 % of the phosphate within 2.5 BV (Figure 6). The maximum concentrations were found 3475 mg N-NH_4^+/L and 2.6 mg P-PO_4^{3-}/L. Pre-concentration factors depends on the volume of solution containing phosphate and ammonium that passed through the column and the volume of NaOH solution required to quantitatively elute the phosphate and ammonium ions from loaded impregnated zeolite. Then, pre-concentration factor is calculated as the ratio of the volumes of the solutions, before and after

extraction (Eq. 20). Pre-concentration factors of 57 and 18 were achieved for ammonium and phosphate, respectively. It is important to point out that manganese and ammonium phosphates are listed as fertilizers and indeed, the zeolites can release nutrients at slow rate, which indicates that results obtained in this study are promising in view of the application of loaded zeolite in N and P from wastewater effluents.

$$P_f \frac{\text{volumes of solutions before extraction}}{\text{volumes of solutions after extraction}} \quad (20)$$

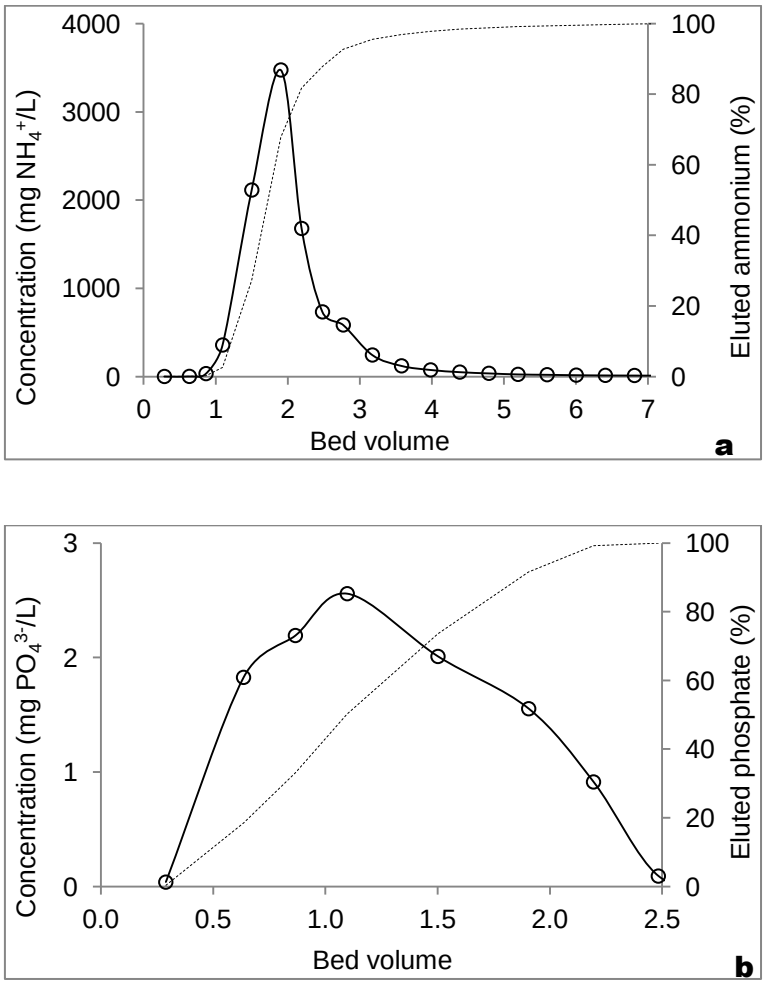

Figure 6. Desorption profiles of a) ammonium and b) phosphate from loaded manganese zeolite (Z-Mn) using 1 M NaOH at 0.4 mL/min.

3.4. Fractionation of immobilized phosphorus in loaded Z-Mn

The residual phosphorus (R-P) and loosely bound phosphorus fraction (LB-P) were found to be 2±1 % and 8±3 %, respectively. The 74±5 % of P was bounded to Al, Fe, Mn hydroxides (Fe+Al+Mn)-P, this fact suggests the participation of hydrated manganese oxide groups in the phosphate immobilization trough ligand exchange complexation. Additionally, the 16±3 % of phosphorus was bounded to calcium, magnesium and manganese (Ca+Mg+Mn)-P fraction. Also the chemical precipitation with cationic species was identified by the XRD analysis (Supplementary material Figure S2).

Conclusions

A hybrid sorbent prepared by impregnation of a natural clinoptilolite zeolite by hydrated manganese oxide in order to remove ammonium and phosphate simultaneously from aqueous solutions. It was observed that ammonium and phosphate sorption capacity were 23 mg/g and 5.6 mg/g, respectively at pH 7.5. The ammonium sorption occurred mainly by ion exchange and complexation due to the hydroxyl groups of the manganese modified hybrid sorbent zeolite (Z-Mn). Moreover, the phosphate removal was accomplished by a combination of electric interactions, inner sphere complexation with ≡Mn-OH functional groups and chemical precipitation (predominantly in the pH range 7 to 9). The XRD analysis of the mineralogical phases precipitated revealed the formation of ammonium manganese phosphate hydrate oxide ($NH_4MnPO_4 \cdot H_2O$). Leaching tests using moderate alkaline bicarbonate solutions shown high availability for both ammonium and phosphate providing a potential use of loaded samples as controlled nutrient release for soil amendments. When evaluated for reuse, the desorption in dynamic conditions and using 1 M NaOH as elution solution provided enrichment factors of 57 and 18 for ammonium and phosphate, respectively.

Acknowledgments

This study has been supported by the WASTE TO PRODUCT project (CTM2014-57302R) financed by Ministry of Science and Innovation and the Catalan government (project ref.

2009SGR905, 2014SGR050). Centro Tecnológico del Agua (CETAQUA), Barcelona Spain for zeolites supply, Secretaría de Educación Superior, Ciencia, Tecnología e Innovación (Senescyt - Ecuador) and Universidad Técnica Particular de Loja - Ecuador (Project - 2014: PROY_QUI_826).

References:

[1] G.J. Millar, A. Winnett, T. Thompson, S.J. Couperthwaite, Equilibrium studies of ammonium exchange with Australian natural zeolites, Journal of Water Process Engineering 9 (2016) 47-57.

[2] X. Yuan, C. Bai, W. Xia, J. An, Acid–base properties and surface complexation modeling of phosphate anion adsorption by wasted low grade iron ore with high phosphorus, J. Colloid Interface Sci. 428 (2014) 208-213.

[3] D. Zhao, A.K. Sengupta, Ultimate removal of phosphate from wastewater using a new class of polymeric ion exchangers, Water Res. 32 (1998) 1613-1625.

[4] A. Gefenienė, D. Kaušpėdienė, J. Snukiškis, Performance of sulphonic cation exchangers in the recovery of ammonium from basic and slight acidic solutions, J. Hazard. Mater. 135 (2006) 180-187.

[5] M. Zhang, H. Zhang, D. Xu, L. Han, D. Niu, B. Tian, J. Zhang, L. Zhang, W. Wu, Removal of ammonium from aqueous solutions using zeolite synthesized from fly ash by a fusion method, Desalination 271 (2011) 111-121.

[6] J.S. Yamani, S.M. Miller, M.L. Spaulding, J.B. Zimmerman, Enhanced arsenic removal using mixed metal oxide impregnated chitosan beads, Water Res. 46 (2012) 4427-4434.

[7] J. Zhu, S.A. Baig, T. Sheng, Z. Lou, Z. Wang, X. Xu, Fe3O4 and MnO2 assembled on honeycomb briquette cinders (HBC) for arsenic removal from aqueous solutions, J. Hazard. Mater. 286 (2015) 220-228.

[8] M.S. Onyango, D. Kuchar, M. Kubota, H. Matsuda, Adsorptive Removal of Phosphate Ions from Aqueous Solution Using Synthetic Zeolite, Ind. Eng. Chem. Res. 46 (2007) 894-900.

[9] B. Pan, J. Wu, B. Pan, L. Lv, W. Zhang, L. Xiao, X. Wang, X. Tao, S. Zheng, Development of polymer-based nanosized hydrated ferric oxides (HFOs) for enhanced phosphate removal from waste effluents, Water Res. 43 (2009) 4421-4429.

[10] M. German, H. Seingheng, A.K. SenGupta, Mitigating arsenic crisis in the developing world: Role of robust, reusable and selective hybrid anion exchanger (HAIX), Sci. Total Environ. 488–489 (2014) 547-553.

[11] N. Haque, G. Morrison, I. Cano-Aguilera, J.L. Gardea-Torresdey, Iron-modified light expanded clay aggregates for the removal of arsenic(V) from groundwater, Microchem. J. 88 (2008) 7-13.

[12] L. Cumbal, J. Greenleaf, D. Leun, A.K. SenGupta, Polymer supported inorganic nanoparticles: characterization and environmental applications, React. Funct. Polym. 54 (2003) 167-180.

[13] C.-S. Jeon, K. Baek, J.-K. Park, Y.-K. Oh, S.-D. Lee, Adsorption characteristics of As(V) on iron-coated zeolite, J. Hazard. Mater. 163 (2009) 804-808.

[14] S. Mustafa, M.I. Zaman, S. Khan, pH effect on phosphate sorption by crystalline MnO2, J. Colloid Interface Sci. 301 (2006) 370-375.

[15] M.J. Jiménez-Cedillo, M.T. Olguín, C. Fall, Adsorption kinetic of arsenates as water pollutant on iron, manganese and iron–manganese-modified clinoptilolite-rich tuffs, J. Hazard. Mater. 163 (2009) 939-945.

[16] M.E. Villanueva, A. Salinas, G.J. Copello, L.E. Díaz, Point of zero charge as a factor to control biofilm formation of Pseudomonas aeruginosa in sol-gel derivatized aluminum alloy plates, Surface and Coatings Technology 254 (2014) 145-150.

[17] K.S. Kim, J.O. Park, S.C. Nam, Synthesis of Iron-loaded Zeolites for Removal of Ammonium and Phosphate from Aqueous Solutions, Environ Eng Res 18 (2013) 267-276.

[18] A.H.M. Hieltjes, L. Lijklema, Fractionation of Inorganic Phosphates in Calcareous Sediments1, J. Environ. Qual. 9 (1980) 405-407.

[19] A. APHA, WEF., Standard methods for the examination of water and wastewater, American Public Health Association, American Water Works Association, and Water Environment Federation, 2000.

[20] H. Valdés, S. Alejandro, C.A. Zaror, Natural zeolite reactivity towards ozone: The role of compensating cations, J. Hazard. Mater. 227–228 (2012) 34-40.

[21] M.K. Doula, Synthesis of a clinoptilolite–Fe system with high Cu sorption capacity, Chemosphere 67 (2007) 731-740.

[22] M.J. Jiménez-Cedillo, M.T. Olguín, C. Fall, A. Colín, Adsorption capacity of iron- or iron–manganese-modified zeolite-rich tuffs for As(III) and As(V) water pollutants, Appl. Clay Sci. 54 (2011) 206-216.

[23] S. Ouvrard, M.-O. Simonnot, M. Sardin, Reactive Behavior of Natural Manganese Oxides toward the Adsorption of Phosphate and Arsenate, Ind. Eng. Chem. Res. 41 (2002) 2785-2791.

[24] M. Kosmulski, Compilation of PZC and IEP of sparingly soluble metal oxides and hydroxides from literature, Adv. Colloid Interface Sci. 152 (2009) 14-25.

[25] S. Mustafa, M.I. Zaman, S. Khan, Temperature effect on the mechanism of phosphate anions sorption by β-MnO2, Chem. Eng. J. 141 (2008) 51-57.

[26] M.I. Zaman, S. Mustafa, S. Khan, B. Xing, Effect of phosphate complexation on Cd2+ sorption by manganese dioxide (β-MnO2), J. Colloid Interface Sci. 330 (2009) 9-19.

[27] M. Król, W. Mozgawa, W. Jastrzębski, K. Barczyk, Application of IR spectra in the studies of zeolites from D4R and D6R structural groups, Microporous and Mesoporous Materials 156 (2012) 181-188.

[28] M. Reháková, Ľ. Fortunová, Z. Bastl, S. Nagyová, S. Dolinská, V. Jorík, E. Jóna, Removal of pyridine from liquid and gas phase by copper forms of natural and synthetic zeolites, J. Hazard. Mater. 186 (2011) 699-706.

[29] A. Alshameri, A. Ibrahim, A.M. Assabri, X. Lei, H. Wang, C. Yan, The investigation into the ammonium removal performance of Yemeni natural zeolite: Modification, ion exchange mechanism, and thermodynamics, Powder Technol. 258 (2014) 20-31.

[30] Z. Luan, J.A. Fournier, In situ FTIR spectroscopic investigation of active sites and adsorbate interactions in mesoporous aluminosilicate SBA-15 molecular sieves, Microporous Mesoporous Mater. 79 (2005) 235-240.

[31] X.-w. Cheng, Y. Zhong, J. Wang, J. Guo, Q. Huang, Y.-c. Long, Studies on modification and structural ultra-stabilization of natural STI zeolite, Microporous Mesoporous Mater. 83 (2005) 233-243.

[32] M.G. Sujana, G. Soma, N. Vasumathi, S. Anand, Studies on fluoride adsorption capacities of amorphous Fe/Al mixed hydroxides from aqueous solutions, J. Fluorine Chem. 130 (2009) 749-754.

[33] H. Huang, X. Xiao, B. Yan, L. Yang, Ammonium removal from aqueous solutions by using natural Chinese (Chende) zeolite as adsorbent, J. Hazard. Mater. 175 (2010) 247-252.

[34] E.B. Simsek, E. Özdemir, U. Beker, Zeolite supported mono- and bimetallic oxides: Promising adsorbents for removal of As(V) in aqueous solutions, Chem. Eng. J. 220 (2013) 402-411.

[35] Y. Su, H. Cui, Q. Li, S. Gao, J.K. Shang, Strong adsorption of phosphate by amorphous zirconium oxide nanoparticles, Water Res. 47 (2013) 5018-5026.

[36] M. Kawashima, Y. Tainaka, T. Hori, M. Koyama, T. Takamatsu, Phosphate adsorption onto hydrous manganese(IV) oxide in the presence of divalent cations, Water Res. 20 (1986) 471-475.

[37] W. Yao, F.J. Millero, Adsorption of Phosphate on Manganese Dioxide in Seawater, Environ. Sci. Technol. 30 (1996) 536-541.

[38] K.Y. Foo, B.H. Hameed, Insights into the modeling of adsorption isotherm systems, Chem. Eng. J. 156 (2010) 2-10.

[39] D. Guaya, C. Valderrama, A. Farran, C. Armijos, J.L. Cortina, Simultaneous phosphate and ammonium removal from aqueous solution by a hydrated aluminum oxide modified natural zeolite, Chem. Eng. J. 271 (2015) 204-213.

[40] M.A. Wahab, H. Boubakri, S. Jellali, N. Jedidi, Characterization of ammonium retention processes onto Cactus leaves fibers using FTIR, EDX and SEM analysis, J. Hazard. Mater. 241–242 (2012) 101-109.

[41] H. Huang, D. Xiao, R. Pang, C. Han, L. Ding, Simultaneous removal of nutrients from simulated swine wastewater by adsorption of modified zeolite combined with struvite crystallization, Chem. Eng. J. 256 (2014) 431-438.

[42] D. Guaya, C. Valderrama, A. Farran, J.L. Cortina, Modification of a natural zeolite with Fe(III) for simultaneous phosphate and ammonium removal from aqueous solutions, J. Chem. Technol. Biot. 91 (2015) 1737–1746.

[43] X. Chen, K. Wendell, J. Zhu, J. Li, X. Yu, Z. Zhang, Synthesis of nano-zeolite from coal fly ash and its potential for nutrient sequestration from anaerobically digested swine wastewater, Bioresource Technol 110 (2012) 79-85.

[44] K. Saltalı, A. Sarı, M. Aydın, Removal of ammonium ion from aqueous solution by natural Turkish (Yıldızeli) zeolite for environmental quality, J. Hazard. Mater. 141 (2007) 258-263.

[45] R. Malekian, J. Abedi-Koupai, S.S. Eslamian, S.F. Mousavi, K.C. Abbaspour, M. Afyuni, Ion-exchange process for ammonium removal and release using natural Iranian zeolite, Appl. Clay. Sci. 51 (2011) 323-329.

[46] A. Alshameri, C. Yan, Y. Al-Ani, A.S. Dawood, A. Ibrahim, C. Zhou, H. Wang, An investigation into the adsorption removal of ammonium by salt activated Chinese (Hulaodu) natural zeolite: Kinetics, isotherms, and thermodynamics, J. Taiwan. Inst. Chem. E. 45 (2014) 554-564.

[47] N. Widiastuti, H. Wu, H.M. Ang, D. Zhang, Removal of ammonium from greywater using natural zeolite, Desalination 277 (2011) 15-23.

[48] M. Sprynskyy, M. Lebedynets, A.P. Terzyk, P. Kowalczyk, J. Namieśnik, B. Buszewski, Ammonium sorption from aqueous solutions by the natural zeolite Transcarpathian clinoptilolite studied under dynamic conditions, J. Colloid. Interf. Sci. 284 (2005) 408-415.

[49] A. Thornton, P. Pearce, S.A. Parsons, Ammonium removal from digested sludge liquors using ion exchange, Water. Res. 41 (2007) 433-439.

[50] J.-W. Choi, S.-Y. Lee, K.-Y. Park, K.-B. Lee, D.-J. Kim, S.-H. Lee, Investigation of phosphorous removal from wastewater through ion exchange of mesostructure based on inorganic material, Desalination 266 (2011) 281-285.

[51] X. You, A. Farran, D. Guaya, C. Valderrama, V. Soldatov, J.L. Cortina, Phosphate removal from aqueous solutions using a hybrid fibrous exchanger containing hydrated ferric oxide nanoparticles, J. Environ. Chem. Eng. 4 (2016) 388-397.

[52] X. You, D. Guaya, A. Farran, C. Valderrama, J.L. Cortina, Phosphate removal from aqueous solution using a hybrid impregnated polymeric sorbent containing hydrated ferric oxide (HFO), J. Chem. Technol. Biot. 91 (2016) 693-704.

[53] H. Yin, Y. Yun, Y. Zhang, C. Fan, Phosphate removal from wastewaters by a naturally occurring, calcium-rich sepiolite, J. Hazard. Mater. 198 (2011) 362-369.

[54] M. Hermassi, C. Valderrama, N. Moreno, O. Font, X. Querol, N. Batis, J.L. Cortina, Powdered Ca-activated zeolite for phosphate removal from treated waste-water, J. Chem. Technol. Biot. 91 (2016) 1962-1971.

[55] N. Hamdi, E. Srasra, Removal of phosphate ions from aqueous solution using Tunisian clays minerals and synthetic zeolite, Journal of Environmental Sciences 24 (2012) 617-623.

[56] S. Moharami, M. Jalali, Removal of phosphorus from aqueous solution by Iranian natural adsorbents, Chem. Eng. J. 223 (2013) 328-339.

[57] W.J. Weber, J.C. Morris, Kinetics of adsorption on carbon solution, J. San. Eng. Div. 89 (1963) 31-59.

[58] L. Lin, Z. Lei, L. Wang, X. Liu, Y. Zhang, C. Wan, D.-J. Lee, J.H. Tay, Adsorption mechanisms of high-levels of ammonium onto natural and NaCl-modified zeolites, Sep. Purif. Technol. 103 (2013) 15-20.

[59] F.G. Helfferich, Ion exchange, McGraw-Hill, New York, 1962.

[60] C. Valderrama, J.I. Barios, M. Caetano, A. Farran, J.L. Cortina, Kinetic evaluation of phenol/aniline mixtures adsorption from aqueous solutions onto activated carbon and hypercrosslinked polymeric resin (MN200), React. Funct. Polym. 70 (2010) 142-150.

[61] G. Moussavi, S. Talebi, M. Farrokhi, R.M. Sabouti, The investigation of mechanism, kinetic and isotherm of ammonia and humic acid co-adsorption onto natural zeolite, Chem. Eng. J. 171 (2011) 1159-1169.

[62] M. Sprynskyy, M. Lebedynets, R. Zbytniewski, J. Namieśnik, B. Buszewski, Ammonium removal from aqueous solution by natural zeolite, Transcarpathian mordenite, kinetics, equilibrium and column tests, Sep. Purif. Technol. 46 (2005) 155-160.